FOREX Publication
Open Access | Rapid and quality publishing

International Journal of
Electrical and Electronics Research (IJEER)
Research Article | Volume 14, Issue 2 | Pages 416-423 | e-ISSN: 2347-470X

Modified Direct Power Control for the Grid-Side Converter of a Wind-Driven PMSG

Ahmed Hassan Adel[1*], Mohammed Fathy Ahmed[1], Ahmed Mohammed Attiya Soliman[1,2], Mohammed Hamouda Ali[1], and Mohammed Shehata Seif[1]

[1]Electrical Engineering Department, Faculty of Engineering Al-Azhar University, Cairo, Egypt
[2]Electrical Engineering Department, College of Engineering, University of Bisha, Saudi Arabia

***Correspondence:** *Ahmed Hassan Adel, ahmed.adel@azhar.edu.eg*

ABSTRACT- This paper presents an improved Direct Power Control (DPC) approach applied to the Grid-Side Converter (GSC) of a wind-driven Permanent Magnet Synchronous Generator (PMSG). The proposed method modifies the conventional switching table by incorporating the errors of the direct and quadrature current components along with the filtered grid voltage vector. The objective is to enhance steady-state behavior and reduce power fluctuations. A comprehensive simulation model is developed in MATLAB/Simulink to assess system performance under different loading conditions and varying wind speeds. Furthermore, the system is evaluated under disturbance conditions, and a comparative validation is performed using classical DPC, Field-Oriented Control (FOC), and Space Vector Pulse Width Modulation (SVPWM)-based FOC. The obtained results confirm that the proposed method achieves improved harmonic and steady-state performance while preserving a relatively simple control structure. Moreover, the Total Harmonic Distortion (THD) of both grid voltage and current remains below 5% at the Point of Common Coupling, complying with IEEE-519 standards. These findings confirm the robustness and effectiveness of the modified DPC scheme in improving power quality and ensuring stable operation of PMSG-based Wind Energy Conversion Systems under variable operating conditions.

Keywords: PMSG, GSC, Wind Energy, DPC, THD.

ARTICLE INFORMATION

Author(s): Ahmed Hassan Adel, Mohammed Fathy Ahmed, Ahmed Mohammed Attiya Soliman, Mohammed Hamouda Ali, and Mohammed Shehata Seif;

Received: 18/02/26; **Accepted**: 09/05/26; **Published**: 25/05/26;
E- ISSN: 2347-470X;
Paper Id: IJEER 1802B11;
Citation: 10.37391/ijeer.140218
Webpage-link:
https://ijeer.forexjournal.co.in/archive/volume-14/ijeer-140218.html

1. INTRODUCTION

The increasing deployment of renewable energy has strengthened the role of wind generation in modern grids. In variable-speed applications, the Permanent Magnet Synchronous Generator (PMSG) is widely adopted due to its efficiency and direct-drive capability. Grid-connected configurations typically use a back-to-back converter composed of a Machine-Side Converter (MSC) and a Grid-Side Converter (GSC). The MSC controls generator dynamics, whereas the GSC manages power exchange with the grid and maintains DC-link voltage stability [1–4].

Several control approaches have been introduced to enhance power regulation and current performance in grid-connected PMSG systems. Among them, Direct Power Control (DPC) has attracted considerable interest due to its fast transient response and relatively simple implementation, as it eliminates the need for inner current control loops and pulse width modulation. Nevertheless, conventional DPC schemes are still affected by variable switching frequency, noticeable power oscillations, and vulnerability to grid disturbances [1, 5].

To address the limitations of classical DPC, several enhanced strategies have been proposed for PMSG-based WECSs. Recent developments have focused on improving switching performance, reducing power ripple, and enhancing harmonic quality through intelligent and modulation-assisted control structures. Approaches based on fuzzy logic, artificial neural networks, and sliding mode control have demonstrated improved dynamic and steady-state performance [1], [6], [7]. In addition, SVM-based, predictive and advanced DPC configurations have been increasingly adopted to achieve fixed switching frequency and better disturbance rejection [8], [9], [10]. Furthermore, recent studies have highlighted the growing integration of modified DPC and advanced MPPT techniques in modern PMSG systems [11].

Although several modified DPC strategies have improved performance, many of them increase algorithmic complexity or depend on additional modulation stages, thereby reducing the inherent simplicity of classical DPC. Unlike existing enhanced DPC methods, the proposed approach preserves the simplicity of classical DPC while improving harmonic performance.

In this study, a modified DPC is proposed for the GSC of a wind-driven PMSG. The switching table is redesigned using three inputs: the direct-axis current error, quadrature-axis

FOREX Publication
Open Access | Rapid and quality publishing
International Journal of Electrical and Electronics Research (IJEER)
Research Article | Volume 14, Issue 2 | Pages 416-423 | e-ISSN: 2347-470X

current error, and the filtered grid-voltage sector obtained via a low-pass filter. This approach enables more accurate voltage-vector selection, leading to improved stability and reduced harmonic distortion without adding computational burden. MATLAB-based simulations demonstrate stable power regulation with THD at the Point of Common Coupling (PCC) maintained below 5%, satisfying IEEE-519 limits under different operating conditions.

The main contributions of this work are summarized as follows:

- Reformulating the classical DPC framework through an alternative control representation that enhances control sensitivity.
- Improving sector identification and switching decision accuracy within the DPC structure.
- Developing a modified switching strategy that enhances steady-state performance without increasing control complexity.

2. SYSTEM MODELING

The investigated configuration includes a wind turbine driving a PMSG, which is interfaced with the electrical grid via a controlled AC-AC converter and an intermediate DC capacitor, as illustrated in *figure 1*.

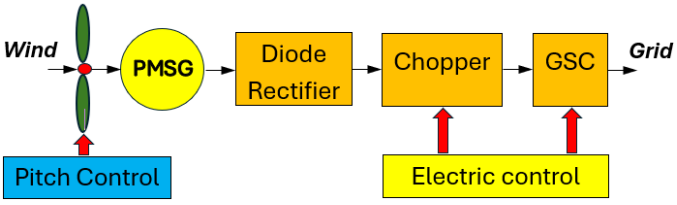

Figure 1. Construction of PMSG-based WECS

The MSC consists of three phase uncontrolled diode rectifier circuit and boost chopper which regulates the generator speed and electromagnetic torque, while the GSC ensures controlled power exchange with the utility grid and maintains the DC-link voltage [12,13].

2.1. Wind Turbine and Pitch Control

The turbine converts wind energy into mechanical torque applied to the PMSG rotor. The aerodynamic power depends on wind speed, air density, rotor swept area, and the power coefficient, which is a function of the tip speed ratio λ and pitch angle β [12]. Below rated wind speed, β is kept near zero to maintain $\lambda \approx \lambda_{opt}$ for maximum power extraction, and the generator operates in MPPT mode. When the wind speed exceeds the rated value, pitch control is activated to increase β, reducing aerodynamic torque and limiting the output power to its rated level. In this region, the turbine operates in power-limiting mode using a PI controller to regulate β based on rotor speed error [14-17].

2.2. PMSG Model

The PMSG is represented in the synchronous dq-reference frame to capture its electromagnetic dynamics. In this frame, the stator voltage components v_d and v_q are expressed as functions of the corresponding current components i_d and i_q, the stator resistance R_s, the flux linkages Ψ_d and Ψ_q, and the electrical angular speed ω_e, as presented in [18-20]. The stator voltage equations are:

$$v_d = R_s i_d + \frac{d\Psi_d}{dt} - \omega_e \Psi_q \quad (1)$$

$$v_q = R_s i_q + \frac{d\Psi_q}{dt} + \omega_e \Psi_d \quad (2)$$

The electromagnetic torque developed by the PMSG is given by [12]:

$$T_e = \frac{3}{2} p\left(i_q \Psi_d - i_d \Psi_q\right) \quad (3)$$

Where p denotes the number of pole pairs. These standard formulations are widely used in PMSG-based WECS studies [21-25].

2.3. Boost Converter & Speed Regulator Interface

The proposed WECS configuration utilizes a cascaded control structure to stabilize the DC-link voltage and enable maximum power tracking, as illustrated in *figure 2*.

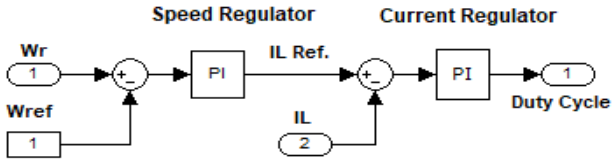

Figure 2. Cascaded control scheme for speed and current regulation

The control scheme consists of two main loops. The outer control loop regulates rotor speed by processing the deviation between the reference speed (ω_{ref}), obtained from the MPPT algorithm, and the measured rotor speed (ω_r). This error is handled by a PI controller to generate the reference inductor current (IL_{ref}), which determines the required electromagnetic torque for optimal power extraction. The inner loop performs current regulation by comparing IL_{ref} with the actual inductor current (IL). The resulting error signal is fed to a second PI controller to compute the duty ratio of the boost converter, ensuring proper current shaping and DC output voltage regulation. This cascaded control scheme ensures a fast and stable dynamic response, allowing the system to maintain the DC-link voltage within desired limits while maximizing the captured energy [26].

2.4. GSC Model and Control Overview

The GSC is modeled as a two-level Voltage Source Converter. The signals controlling the gates of the converter are determined by the proposed Modified DPC strategy, which bases decision-making on the direct and quadrature current errors (H_d, H_q) and the filtered grid voltage sector S. Since the control law does not rely explicitly on instantaneous calculation of active and reactive powers, the detailed converter output voltage equations are omitted, and the

FOREX Publication
Open Access | Rapid and quality publishing
International Journal of Electrical and Electronics Research (IJEER)
Research Article | Volume 14, Issue 2 | Pages 416-423 | e-ISSN: 2347-470X

converter is instead implemented in simulation with controlled voltage sources as per switching decisions.

Two common control strategies are widely used for the GSC in PMSG-based wind energy systems: Field Oriented Control (FOC) and DPC. In FOC, the converter currents are controlled in a rotating reference frame based on PWM to control the active and reactive power components independently, providing smooth and accurate control but with higher complexity [27, 28]. In contrast, DPC directly controls the instantaneous values of active and reactive powers using a switching lookup table based on the measured voltages and currents, which eliminates the need for PWM and current controllers, offering a simpler structure and faster dynamic response [1, 5].

3. PROPOSED MODIFIED DPC METHOD

3.1. Motivation and Concept

Although the classical Direct Power Control offers a simple structure and fast dynamic response, it suffers from significant power ripples, variable switching frequency, and sensitivity to grid voltage distortion [1, 5]. To address these drawbacks while maintaining the simplicity of classical DPC, a Modified DPC (MDPC) strategy is proposed in this paper.

The main contribution of the proposed method is the introduction of a new switching table based on direct and quadrature current component errors instead of instantaneous power errors, combined with a filtered grid voltage sector for improved voltage vector selection. This modification enhances stability, reduces total harmonic distortion (THD), and provides smoother control action at the PCC.

3.2. Modified Control Structure

The proposed MDPC maintains the same overall control framework as classical DPC but introduces three key improvements in the decision layer, as illustrated in *figure 3*.

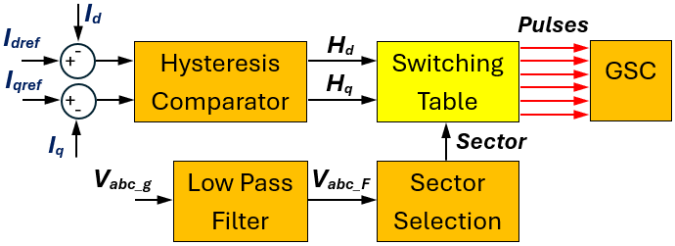

Figure 3. Block diagram of the proposed MDPC

3.2.1. Current-Error-Based Decision Variables

Instead of comparing instantaneous active and reactive powers, the proposed strategy uses the direct component error (Δi_d) and quadrature component error (Δi_q) as the main control variables.

These errors are given by:

$$\Delta i_d = i_{dr} - i_d \quad (4)$$

$$\Delta i_q = i_{qr} - i_q \quad (5)$$

Where; i_d , i_q are direct and quadrature components of the grid current in the two-axis rotating reference frame. The reference value of the direct-axis current (i_{dr}) is obtained by a DC-bus voltage PI regulator, which maintains the DC-link voltage at its rated value. On the other hand, the quadrature-axis current reference (i_{qr}) is obtained through a reactive power regulator followed by a voltage regulator, ensuring proper control of the reactive power and terminal voltage.

Using current components directly provides faster error detection and more accurate control over the converter output voltage vector.

3.2.2. Filtered Grid Voltage Sector Identification

A Low-Pass Filter is used to reduce harmonic distortion and high-frequency noise of the instantaneous grid voltage. The filtered voltage is then used to determine the voltage sector (1–6), ensuring robust operation even under grid distortion or measurement noise.

The voltage angle is determined using the following equation:

$$\theta = \sin^{-1} \frac{v_\beta}{\sqrt{{v_\alpha}^2 + {v_\beta}^2}} \quad (6)$$

where v_α and v_β refer to the filtered voltage components in 2-phase stationary frame obtained using Clarke transformation.

This modification minimizes the risk of incorrect sector detection, which is a common issue in conventional DPC under unbalanced or distorted grid conditions.

3.2.3. Modified Switching Table

In a two-level voltage source inverter employed for a direct power controller, eight discrete voltage vectors are produced according to the switching states of the inverter legs. Six active vectors form a hexagonal structure in the α–β frame and control the instantaneous active and reactive power, the two remaining vectors are zero vectors and located at the origin and help maintain the power within the hysteresis bands [29].

A modified switching table is introduced based on the values of ($\Delta i_d, \Delta i_q$) and the filtered grid voltage sector. The table determines the optimal switching state of the converter ($v_0 - v_7$) to bring the current components toward their references while minimizing ripple. The general structure of the modified table is similar to that of the classical DPC, but the control decisions are now current-oriented rather than power-oriented. The detailed proposed table is provided in *table 1*.

Table 1. Proposed Switching table

Hiq	Hid	S1	S2	S3	S4	S5	S6
1	1	V6	V1	V2	V3	V4	V5
	0	V7	V0	V7	V0	V7	V0
	-1	V1	V2	V3	V4	V5	V6
-1	1	V4	V5	V6	V1	V2	V3
	0	V7	V0	V7	V0	V7	V0
	-1	V2	V3	V4	V5	V6	V1

FOREX Publication
Open Access | Rapid and quality publishing
International Journal of Electrical and Electronics Research (IJEER)
Research Article | Volume 14, Issue 2 | Pages 416-423 | e-ISSN: 2347-470X

There are six sectors determine the position of the filtered grid voltage, each spanning 60°. Sector 1 covers the interval from 0° to 60°, while the remaining sectors are arranged sequentially.

The proposed control strategy is based on regulating the d–q axis current components by minimizing the current errors. The error between the reference and measured currents is processed by the controller to generate the required voltage components. As a result, the current error dynamics are driven toward zero, ensuring accurate tracking of the reference values. Since identical controller tuning is applied, similar transient responses are observed among the methods, while the main improvement of the proposed approach is reflected in steady-state performance and ripple reduction. This current-based regulation indirectly ensures proper control of active and reactive power. Simulation results presented in the following Section confirm that the proposed MDPC achieves superior performance compared to classical DPC under variable conditions.

4. SIMULATION MODEL AND RESULTS DISCUSSION

4.1. Simulation Model

To validate the performance of the proposed Modified DPC (MDPC) strategy, a detailed model of a 2 MW PMSG-based WECS was developed in MATLAB/Simulink. *figure 4* illustrates the Simulink diagram of grid-connected PMSG.

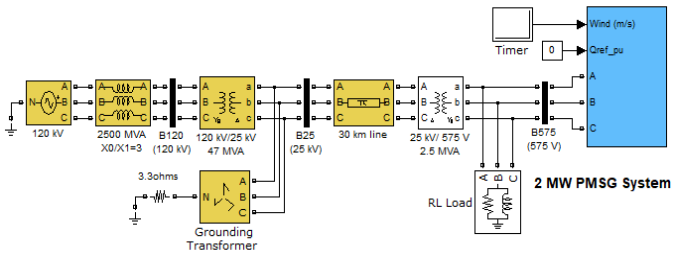

Figure 4. Configuration of the studied grid-connected PMSG system

As shown in *figure 4*, the generator is connected to a 60 Hz-grid via B575 bus bar or PCC. The system parameters were selected according to typical industrial ratings. The parameters of the generator that used in the simulation are given in *table 2* and summarized as follows:

Table 2. Generator's Parameters

Parameter	Value
Rated power	2 MW
Line-line voltage	730 V
Pole pairs	32
Inertia constant	0.62 s
Friction factor	0.01 pu
Stator resistance; Rs	0.006 pu
Direct-axis reactance	0.174 pu
Quadrature-axis reactance	0.0632 pu

The per unit values are calculated according to base values of 730 V and 2.22 MVA, considering a power factor of 0.9. The generator is connected to the grid through a 0.1 mH filter. Wind turbine parameters are given in *table 3*. The controllers' gains are provided in *Appendix A*, in *Table A1*.

Table 3. Wind Turbine Parameters

Parameter	Value
Rated wind speed	12.4 m/s
Cut-in speed	6 m/s
Cut-off speed	30 m/s
Air density	1.225 kg/m³
Blade radius	45 M
Turbine inertia constant	4.32 S
Power coefficient (max)	0.45

The simulation was carried out under steady wind speed corresponding to rated mechanical power, and the results were analyzed at the PCC. Loads of 1 and 2 MW were considered at a lagging power factor of 0.95, and the no-load condition was also considered in the analysis.

In addition, for validation purposes, the simulation study includes four control strategies, namely classical DPC, the proposed MDPC, FOC, and SVM-based FOC, all implemented under identical operating conditions.

4.2. Dynamic Performance Analysis

4.2.1. Analysis at constant speed

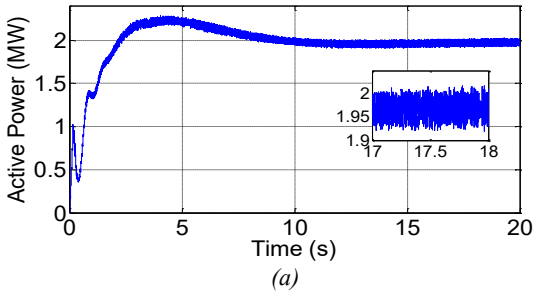

(a)

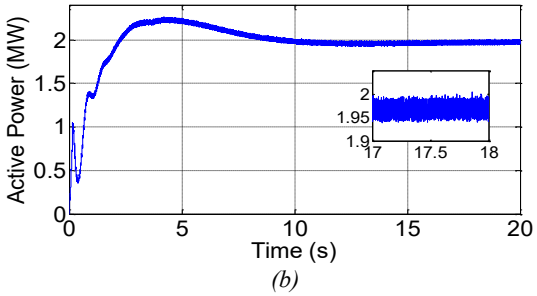

(b)

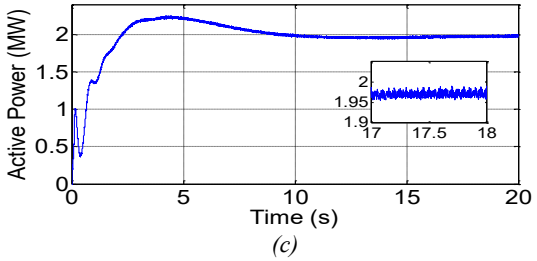

(c)

FOREX Publication
Open Access | Rapid and quality publishing
International Journal of Electrical and Electronics Research (IJEER)
Research Article | Volume 14, Issue 2 | Pages 416-423 | e-ISSN: 2347-470X

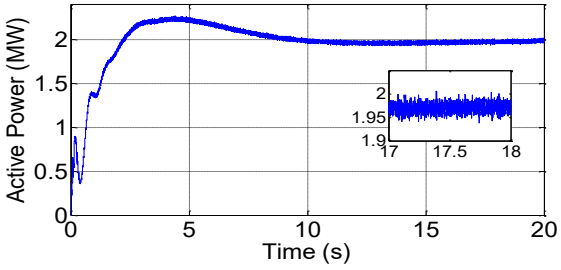

(d)

Figure. 5 Generator active power at 2 MW load and 13 m/s speed for: (a) DPC; (b) MDPC; (c) FOC; (d) SVM

Figure 5 depicts the active power response for the different control strategies. All methods exhibit a unified dynamic behavior, characterized by a settling time of 8.5s and an overshoot of 12.5%. This identical transient performance is primarily governed by the high mechanical inertia of the 2MW PMSG and the consistent tuning of the outer DC-voltage loop. However, as summarized in *table 5*, a clear distinction emerges in the steady-state phase. The Classical DPC suffers from the highest power ripple (4.84%), whereas the Proposed MDPC significantly suppresses these oscillations to 3.31%.

While FOC and SVM techniques maintain the lowest ripple profiles, the MDPC achieves a significant reduction in power oscillations compared to the classical DPC. This performance enhancement demonstrates that the MDPC can mitigate the inherent drawbacks of conventional DPC while preserving its characteristic dynamic response, making it a competitive alternative for high-power quality requirements.

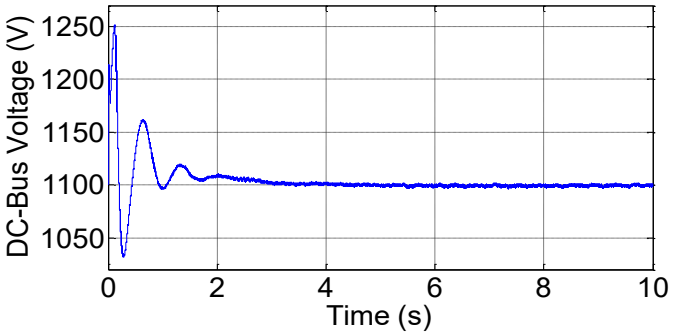

(a)

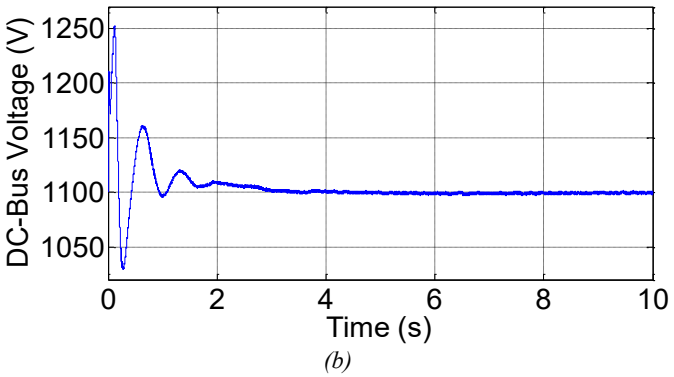

(b)

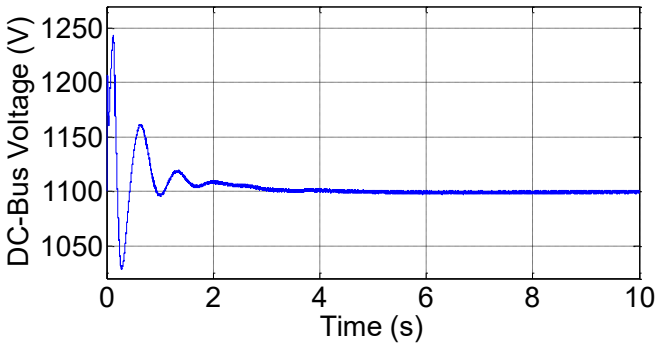

(c)

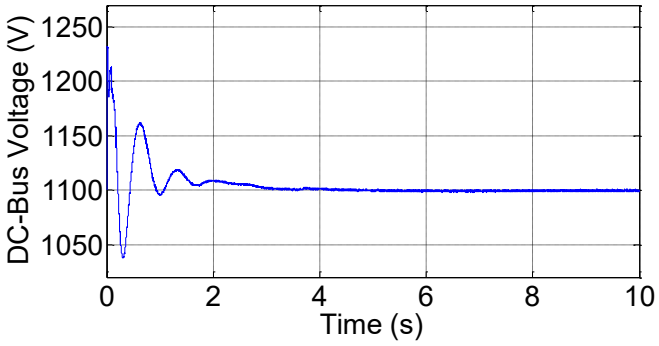

(d)

Figure. 6 DC-bus voltage at 2 MW load and 13 m/s speed for: (a) DPC; (b) MDPC; (c) FOC; (d) SVM

The DC-link voltage response is illustrated in *figure 6*. All strategies succeed in maintaining the DC voltage at its reference level with a fast recovery time. According to the quantitative analysis in *table 5*, the Proposed MDPC exhibits improved regulation compared to both Classical DPC and FOC. Specifically, the MDPC reduces the voltage ripple to 0.286%, a noticeable improvement over the 0.376% and 0.323% recorded for Classical DPC and FOC, respectively. Although the SVM-based approach maintains the lowest ripple (0.189%) due to its fixed switching frequency, the MDPC offers a more stable DC-link voltage than the FOC. This enhancement contributes to the longevity of the capacitor bank and supports a high-quality power injection into the grid with minimized harmonic distortions.

4.2.2. System Response Under Grid Fault and Variable Wind Speed

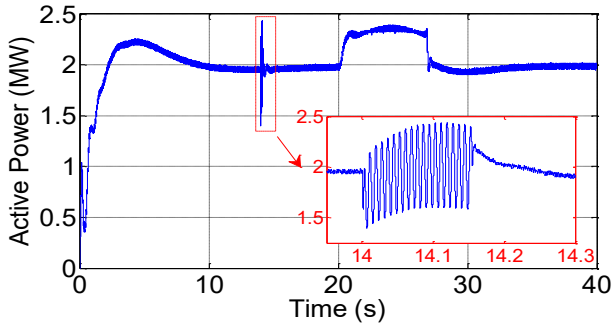

Figure. 7 Active power response at 1MW load under SLG fault and variable wind speed conditions

FOREX Publication
Open Access | Rapid and quality publishing
International Journal of Electrical and Electronics Research (IJEER)
Research Article | Volume 14, Issue 2 | Pages 416-423 | e-ISSN: 2347-470X

The dynamic performance and robustness of the PMSG-based wind energy system are evaluated under severe disturbances, as illustrated in *figure 7*. Initially, the system operates at a rated wind speed of 13 m/s, delivering 2 MW of active power to a 1 MW local load at the PCC, with the surplus power being exported to the utility grid. At t=14 s, a Single Line-to-Ground (SLG) fault is initiated at the PCC for 9 cycles with a low fault resistance of 0.01 Ω. The magnified inset reveals high-frequency oscillations during the fault, with a peak transient overshoot of approximately 2.43 MW. Despite this momentary surge, the controller demonstrates superior damping, restoring stability promptly upon clearance.

At t=20 s, the system's adaptability is tested by increasing the wind speed to 15 m/s. The active power output exhibits a transient overshoot, reaching approximately 2.38 MW. This peak is a realistic consequence of the mechanical inertia and the response time of the pitch actuators. However, this temporary increase does not compromise system integrity, as the pitch angle control successfully intervenes at t=27 s to regulate the power back to its rated 2 MW. This ensures that the PMSG operates within safe thermal and mechanical limits while maintaining reliable power sharing between the local load and the grid.

4.3. Harmonic Performance (THD Analysis)

The THD of the waveforms of both voltage and current at the PCC was evaluated using the Fast Fourier Transform (FFT) tool in Simulink. THD is calculated relative to fundamental. The results for the proposed method are illustrated in *figure 8(a)* and *(b)*, which present the harmonic analysis of the current and voltage at the PCC, respectively, under a load of 2 MW and a 0.95 lagging power factor.

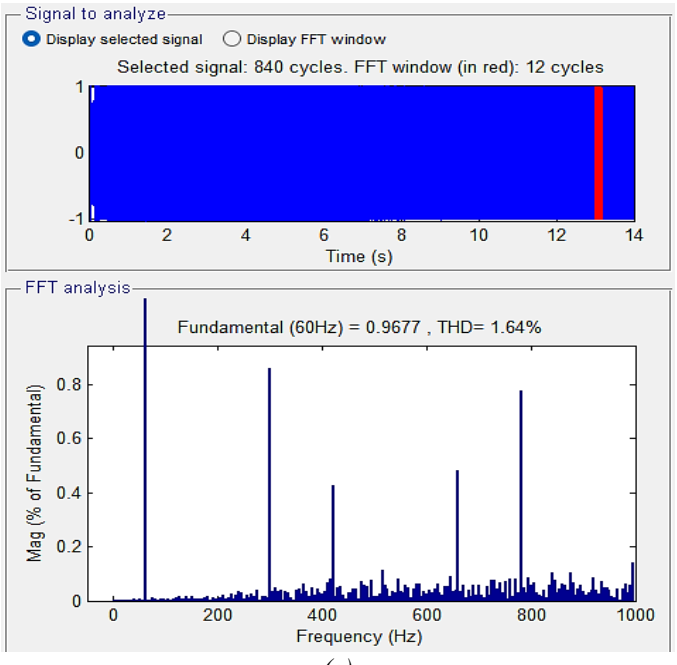

(a)

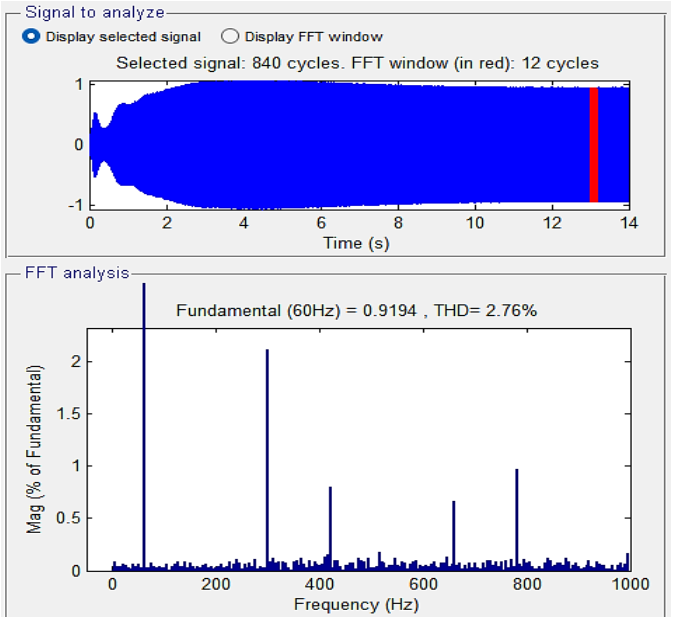

(b)

Figure 8. THD analysis of the proposed MDPC at 2MW load for: (a) Voltage; (b) Current

As shown in *figure 8(a)*, the current THD is recorded at 2.76%, with a fundamental component of 0.9194, reflecting efficient power conversion despite the presence of the 5th harmonic at approximately 2.1%. Conversely, *figure 8(b)* illustrates a superior harmonic profile for the grid voltage, where the THD drops to 1.64% and the fundamental magnitude improves to 0.9677. The comparative analysis of both figures highlights the system's robust voltage regulation and the effectiveness of the filtering stage in suppressing converter-induced distortions. Ultimately, both profiles remain well within the permissible limits of the IEEE 519 standard, ensuring high-quality power injection into the utility grid.

The THD values were evaluated, for the proposed method, under different load conditions and variable wind speeds. The following *table 4* summarizes the measured THD values under different operating conditions.

Table 4. THD values for the proposed method

Condition/ THD%	Voltage	Current
No load & 13m/s	3.65	3.88
1MW & 13m/s	2.21	3.00
1MW & 15m/s	2.25	2.94
2MW & 13m/s	1.64	2.76

It is observed from the table that as the load increases, the THD of both voltage and current decreases noticeably. This indicates that higher loading improves the waveform quality and reduces the harmonic content due to the better utilization of the converter switching states. The THD values of voltage and current are well below the IEEE 519-2014 recommended limit of 5% [30]. A comparison of the proposed method with other existing techniques is provided in *table 5*.

FOREX Publication
Open Access | Rapid and quality publishing
International Journal of Electrical and Electronics Research (IJEER)
Research Article | Volume 14, Issue 2 | Pages 416-423 | e-ISSN: 2347-470X

4.4. Comparative Performance Analysis

Table 5. Comparative performance of different control methods

Method	THD (1MW) %	THD (2MW) %	Power Ripple %	V_{DC} Ripple %	V_{DC} Overshoot %
DPC	3.86	3.82	4.84	0.376	8.9
MDPC	3.00	2.76	3.32	0.286	8.9
FOC	1.75	2.18	1.93	0.323	8.2
SVM	1.76	0.63	3.18	0.189	7.1

Table 5 presents a comparative performance analysis of the investigated control strategies. All parameters were evaluated at a wind speed of 13 m/s and a 2 MW load at the PCC, with THD also calculated for a 1 MW load condition. The proposed MDPC method significantly improves performance compared to classical DPC, reducing the current THD by approximately 22% at 1 MW and 28% at 2 MW. In addition, the power ripple and DC-link voltage ripple are reduced by about 31% and 24%, respectively. Moreover, an SVM-based method is included as an advanced technique, showing the lowest harmonic distortion. Although FOC achieves the minimum ripple, the proposed method provides a comparable performance with a simpler implementation. Overall, the proposed approach offers a good trade-off between performance and complexity.

The presented results are based on a detailed simulation model with realistic parameters; however, experimental validation will be considered in future work.

5. CONCLUSIONS

This work presented the implementation and performance evaluation of a modified Direct Power Control strategy for a 2 MW PMSG grid-connected system. The proposed scheme demonstrated satisfactory dynamic response, precise power regulation, and robust DC-link stability. Under various loading conditions and wind speeds, the system consistently achieved steady-state operation within 8.5s with negligible error.

To verify the design's robustness, a comparative analysis and disturbance testing were conducted against classical DPC and FOC-based methods. The results highlight that the modified switching table ensures smoother voltage-vector transitions and significantly reduces instantaneous power ripples. Regarding power quality, the measured THD for both voltage and current remained strictly within IEEE 519 limits, with performance further improving at higher power levels.

Furthermore, the proposed strategy is computationally efficient, requiring fewer control parameters than advanced methods like predictive DPC or SVM. Overall, this modified DPC offers a robust, cost-effective, and power-quality-compliant solution for wind-driven PMSG systems, maintaining high stability across a wide range of operating conditions.

Appendix A

Table A1. Control Parameters for controllers

Controller	Parameter	Value
Pitch controller	*Kp*	15
DC bus voltage regulator	*Kp, Ki*	1.1, 27.5
Var regulator	*Ki*	0.05
Voltage regulator	*Ki*	2
Speed regulator	*Kp, Ki*	5, 1
Boost current regulator	*Kp, Ki*	0.025, 10
Hysteresis comparator	Bandwidth	0.01(pu)

Author Contributions: Conceptualization, A.H.A. and M.S.S.; methodology, A.H.A. and A.M.A.S.; software, A.H.A.; validation, M.F.A. and M.H.A.; formal analysis, A.H.A. and M.H.A.; investigation, A.H.A. and A.M.A.S.; data curation, M.H.A.; writing—original draft preparation, A.H.A.; writing—review and editing, M.F.A. and M.S.S.; visualization, A.H.A.; supervision, M.F.A. and M.S.S.; project administration, M.S.S. All authors have read and agreed to the published version of the manuscript.

Funding Source: "This research received no external funding"

Conflicts of Interest: "The authors declare no conflict of interest."

REFERENCES

[1] B. Majout, H. El Alami, H. Salime, N. Z. Laabidine, Y. El Mourabit, S. Motahhir, M. Bouderbala, M. Karim, and B. Bossoufi, "A review on popular control applications in wind energy conversion system based on permanent magnet generator (PMSG)," Energies, vol. 15, no. 17, pp. 1-41, Aug. 2022, doi:10.3390/en15176238.

[2] A. Raouf, H. Ijaz, S. Khan, and M. Iqbal, "Wind energy conversion systems based on a synchronous generator: comparative review," Energies, vol. 16, no. 5, pp. 1-25, Mar. 2023, doi: 10.3390/en16052147.

[3] N. Hassan, K. A. El_Atey and A. H. M. El-Enany, "Economically optimal design of hybrid renewable energy systems using HOMER and ACO," Journal of Al-Azhar University Engineering Sector, vol. 13, no. 48, pp. 1016–1030, 2018, doi:10.21608/auej.2018.18977.

[4] V. M. Pham, "Control for Wind Turbine System using PMSG when Wind Speed Changes," International Journal of Electrical and Electronics Research (IJEER), vol. 12, no. 2, pp. 520-528, May 2024,doi:10.37391/IJEER.120225.

[5] R. Mishra and T. K. Saha, "Predictive power control of PMSG based WECS: development and implementation for smooth grid synchronisation, balanced and unbalanced grid," Mathematics and Computers in Simulation, vol. 215, pp. 323–337, Jan. 2024, doi:10.1016/j.matcom.2023.08.011.

[6] H. Salime et al., "A novel combined FFOC-DPC control for wind turbine based on the permanent magnet synchronous generator," Energy Reports, vol. 9, pp. 3204–3221, Oct. 2023, doi:10.1016/j.egyr.2023.02.012.

[7] O. Hachana, B. Meghni, A. Benamor, and I. Toumi, "Efficient PMSG wind turbine with energy storage system control based shuffled complex evolution optimizer," ISA Transactions, vol. 131, pp. 377–396, Dec. 2022, doi:10.1016/j.isatra.2022.05.014.

[8] M. A. Hannan, M. S. Hossain Lipu, A. Hussain, M. M. Islam, and A. Ayob, "Wind energy conversions, controls, and applications," Sustainability, vol. 15, no. 5, p. 3986, 2023, doi:10.3390/su15053986.

[9] R. Sharma, K. Sahay, and S. Singh, "Control aspects for PMSG-based grid-connected wind energy conversion systems – a review," SSRG International Journal of Electrical and Electronics Engineering, vol. 10, no. 12, pp. 72-86, Dec. 2023, doi:10.14445/23488379/IJEEE-V10I12P108.

International Journal of Electrical and Electronics Research (IJEER)
Research Article | Volume 14, Issue 2 | Pages 416-423 | e-ISSN: 2347-470X

[10] M. A. Mossa, R. A. Mohamed and A. S. Al-Sumaiti, "Performance Enhancement of a Grid Connected Wind Turbine-Based PMSG Using Effective Predictive Control Algorithm," in IEEE Access, vol. 13, pp. 64160-64185, 2025, doi:10.1109/ACCESS.2025.3557194.

[11] X. C. Le, M. Q. Duong, and K. H. Le, "Review of the modern maximum power tracking algorithms for permanent magnet synchronous generator of wind power conversion systems," Energies, vol. 16, no. 1, p. 402, 2023, doi:10.3390/en16010402.

[12] R. A. Ibrahim and N. E. Zakzouk, "A PMSG wind energy system featuring low-voltage ride-through via mode-shift control," Applied Sciences, vol. 12, no. 3, p. 964, 2022, doi:10.3390/app12030964.

[13] B. N. Reddy, R. Jalli, K. S. Prudhviraj, K. B. Shetty, Ch. Rami Reddy, H. Kotb, A. Emara, and M. Alruwaili, "Wind turbine with line-side PMSG fed DC-DC converter for voltage regulation," PLOS ONE, vol. 19, no. 6, e0305272, 2024, doi:10.1371/journal.pone.0305272.

[14] L. Li, X. Deng, Y. Liu, X. Yue, H. Wang, R. Liu, Z. Cai, and R. Cai, "Research on nonlinear pitch control strategy for large wind turbine units based on effective wind speed estimation," Electronics, vol. 14, no. 12, p. 2460, 2025, doi:10.3390/electronics14122460.

[15] S. Musuroi, "Experimental determination of the power coefficient and energy-efficient operating zone for a 2.5 MW wind turbine under high-wind conditions," Energies, vol. 18, no. 18, p. 4912, 2025, doi:10.3390/en18184912.

[16] M. Khaled, M. K. Ahmed, M. Elwany and M. Shalaby, "MPPT of small wind turbine direct-drives axial flux permanent magnet synchronous generator," Journal of Al-Azhar University Engineering Sector, vol. 14, no. 52, pp. 968–981, 2019, doi:10.21608/auej.2019.43481.

[17] O. E. Abdellatif, "Investigating robust pitch angle control techniques of the NREL 1.5 MW HAWT," Journal of Al-Azhar University Engineering Sector, vol. 20, no. 74, pp. 211–227, 2025, doi:10.21608/auej.2024.309648.1696.

[18] A. G. Abo-Khalil and M. Alobaid, "Optimized control for PMSG wind turbine systems under unbalanced and distorted grid voltage scenarios," Sustainability, vol. 15, no. 12, p. 9552, 2023, doi:10.3390/su15129552.

[19] V. V. Yadav and S. Balasubramaniyan, "Synchronization stability and control strategies for PMSG-based wind energy systems under grid fault conditions," Energy Reports, vol. 13, pp. 6148–6160, May 2025, doi:10.1016/j.egyr.2025.05.052.

[20] Y. Barradi, K. Zazi, M. Zazi, and N. Khaldi, "Control of PMSG based variable speed wind energy conversion system connected to the grid with PI and ADRC approach," International Journal of Power Electronics and Drive Systems, vol. 11, no. 2, pp. 953–968, June 2020, doi:10.11591/ijpeds.v11.i2.

[21] A. Tobias-Gonzalez, R. Pena-Gallardo, J. Morales-Saldana, A. Medina-Rios, and O. Anaya-Lara, "A state-space model and control of a full-range PMSG wind turbine for real-time simulations," Electrical Engineering, vol. 100, pp. 1825-1840, 2018, doi:10.1007/s00202-018-0691-y.

[22] A. E. Elngar, A. S. Sabik, A. H. Adel, and A. S. Nada, "Comparative performance evaluation of wind energy systems using doubly fed induction generator and permanent magnet synchronous generator," Wind, vol. 5, no. 4, p. 31, Nov. 2025, doi:10.3390/wind5040031.

[23] A. Gencer, " Modelling and control of permanent magnet synchronous generator based on three level NPC using fuzzy PI," Balkan Journal of Electrical and Computer Engineering, vol. 6, no. 3, pp. 172-177, 2018, doi:10.17694/bajece.423464.

[24] P. Acharya, A. Papadakis, and M. N. Shaikh, "Modelling and design of a 3kW permanent magnet synchronous generator suitable for variable speed small wind turbines." MATEC web of conferences. Vol. 55. EDP Sciences, 2016, doi:10.1051/matecconf/20165504001.

[25] Z. Hamodat, I. K. Hussein, and B. A. Nasir, "An accurate efficiency calculation for PMSG utilized in renewable energy systems," Journal of Robotics and Control (JRC), vol. 4, no. 4, pp. 458–465, July 2023, doi:10.18196/jrc.v4i4.18441.

[26] H. H. H. Mousa, A. R. Youssef, and E. E. M. Mohamed, "Optimal power extraction control schemes for five-phase PMSG based wind generation systems," Engineering Science and Technology, an International Journal, vol. 23, no. 1, pp. 144–155, Feb. 2020, doi:10.1016/j.jestch.2019.04.004.

[27] M. A. Mostafa, E. A. El-Hay, and M. M. Elkholy, "Recent trends in wind energy conversion system with grid integration based on soft computing methods: comprehensive review, comparisons and insights," Arch. Comput. Methods Eng., vol. 30, pp. 1439-1478, 2023, doi:10.1007/s11831-022-09842-4.

[28] G. H. Ghanayem, M. Alathamneh, and R. M. Nelms, "PMSM field-oriented control with independent speed and flux controllers for continuous operation under open-circuit fault at light load conditions," Energies, vol. 17, no. 3, p. 593, 2024, doi:10.3390/en17030593.

[29] H. Chae and C. Roh, "Enhanced output performance of two-level voltage source inverters using simplified model predictive control with multi-virtual-voltage vectors," Machines, vol. 12, no. 11, p. 781, 2024, doi:10.3390/machines12110781.

[30] IEEE Std 519-2014, IEEE Recommended Practice and Requirements for Harmonic Control in Electric Power Systems, IEEE Power and Energy Society, 2014.